

Temporal Parallelization of Inference in Hidden Markov Models

Syeda Sakira Hassan, Simo Särkkä, *Senior Member, IEEE*, and Ángel F. García-Fernández

Abstract—This paper presents algorithms for parallelization of inference in hidden Markov models (HMMs). In particular, we propose parallel backward-forward type of filtering and smoothing algorithm as well as parallel Viterbi-type maximum-a-posteriori (MAP) algorithm. We define associative elements and operators to pose these inference problems as parallel-prefix-sum computations in sum-product and max-product algorithms and parallelize them using parallel-scan algorithms. The advantage of the proposed algorithms is that they are computationally efficient in HMM inference problems with long time horizons. We empirically compare the performance of the proposed methods to classical methods on a highly parallel graphical processing unit (GPU).

Index Terms—parallel forward-backward algorithm, parallel sum-product algorithm, parallel max-product algorithm, parallel Viterbi algorithm

I. INTRODUCTION

HIDDEN Markov models (HMMs) have gained a lot of attention in last two decades due to their simplicity and broad range of applications [1]–[5]. Successful real-world application areas of HMMs include speech recognition, decoding of convolutional codes, target tracking and localization, facial expression recognition, gene prediction, gesture recognition, musical composition, and bioinformatics [1], [6]–[11]. An HMM is a statistical model that provides a simple and flexible framework that can express the conditional independence and joint distributions using graph-like structures. An HMM can be thought of as a specific form of a probabilistic graphical model consisting of two components: a structural component that defines the *edges* and a parametric component that encodes *potentials* associated with the edges in the graph. A graphical representation of an HMM is shown in Fig. 1. An HMM is a doubly stochastic process where the underlying stochastic process (light gray-colored nodes) can only be observed through another stochastic process (dark gray-colored nodes) [1], [12]. One of the primary tasks in graphical models is the process of computing marginals and conditional probability distributions, the *inference* task, which is a computationally intensive procedure.

If the HMM model has D states and the sequence of length is T , then there are D^T possible state sequences. For the classical algorithms, such as forward-backward and

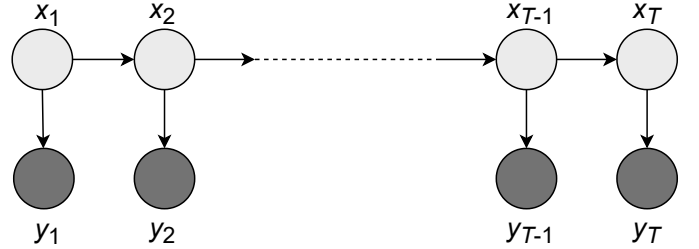


Fig. 1. A hidden Markov model (HMM). The observed nodes are shaded in dark gray whereas unobserved nodes are in light gray.

Viterbi algorithms, the time complexity is $O(D^2T)$ to find the marginals, or alternatively, the most likely sequence, known as the *Viterbi* path [1], [6], [13]. Some methods to speed up these algorithms, also using parallelization, have already appeared in literature. For instance, Lifshits et al. [14] used a compression scheme by exploiting the repetitive patterns in the observed sequences to speed up the inference task. Sand et al. [15] developed a parallel forward algorithm using SIMD instructions and multiple cores. Nielsen and Sand [16] presented a parallel reduction on forward algorithm. Chatterjee and Russell [17] used the temporal abstraction concept from dynamic programming to speed up the Viterbi algorithm. Using accelerated hardware, tile-based Viterbi algorithm was proposed by [18] where the matrix multiplication was done in parallel. Maleki et al. [19] proposed an optimized method to solve a particular class of dynamic programming problems by tropical semiring. They showed that this can be used to optimize the Viterbi algorithm. Nevertheless, parallelization has not been fully investigated in HMM inference tasks. In this paper, we develop novel algorithms which can achieve $O(\log T)$ span complexity in forward-backward and Viterbi algorithms.

Over the last half a century, numerous parallel algorithms have been developed, and these algorithms can take advantage of the acceleration power of specialized hardware accelerators such as general purpose *graphical processing units* (GPUs) [20], *neural processing units* (NPU) [21], and *tensor processing units* (TPUs) [22]. These accelerators allow for parallel computation on large amounts of data, making computation faster and cheaper, and therefore economically viable. Among these accelerators, GPUs are most widely used. The GPU architecture allows for massive parallelization of general-purpose algorithms [23]. Table I summarizes few recent works on the inference tasks of HMM, which were implemented on GPU. However, these works were optimized particularly for

S. Hassan and S. Särkkä are with the Department of Electrical Engineering and Automation, Aalto University, 02150 Espoo, Finland (emails: syeda.s.hassan@aalto.fi, simo.sarkka@aalto.fi).

Ángel F. García-Fernández is with the Department of Electrical Engineering and Electronics, University of Liverpool, Liverpool L69 3GJ, United Kingdom (email: angel.garcia-fernandez@liverpool.ac.uk). He is also with the ARIES Research Centre, Universidad Antonio de Nebrija, Madrid, Spain.

speech recognition tasks and did not explore the full capabilities of parallelism. In order to utilize parallelism, the sequential algorithms need to be adapted to the primitive operations that allow for parallel execution on parallel platforms. For example, the all-prefix-sums, also known as parallel-scan algorithm [24], [25] can be used to run computations in parallel provided that they can be formulated in terms of binary associative operations.

TABLE I
PREVIOUS WORKS ON HMM INFERENCE TASK USING GPU. THE NOTATION ‘-’ MEANS THAT THE VALUE WAS NOT MENTIONED IN THE ORIGINAL PAPER.

Algorithm	States	Observations	Speed improvement
Forward-backward [26]	8	200	3.5x
Forward [27]	512	3-10	880x
Baum-Welch [27]	512	3-10	180x
Viterbi [28]	-	2000-3000	3x
Forward [29]	4000	1000	4x
Baum-Welch [29]	4000	1000	65x

Recently, the parallel-scan algorithm has been used in parallel Bayesian filtering and smoothing algorithms to speed up the sequential computations via parallelization [30], [31]. Although this framework is applicable to HMMs as well, the difference to our proposed framework is that here we formulate the inference problem in terms of potentials. This results in different backward pass in the algorithm which corresponds to two-filter smoother formulations, whereas the formulation in [30], [31] is of Rauch–Tung–Striebel type smoother [32]. In the present article, we also consider parallel Viterbi-type MAP algorithm which has not been explored before.

The main contribution of this paper is to present a parallel framework to perform the HMM inference tasks efficiently by using the parallel-scan algorithm. In particular, we formulate the sequential operations of sum-product and max-product algorithms as binary associative operations. This formulation allows us to construct parallel versions of the forward-backward algorithm and the Viterbi algorithm with $O(\log T)$ span complexity. For latter algorithm, we propose two alternative parallelization: the path-based and forward-backward based formulation. We also empirically evaluate the computational speed advantage of these methods on a GPU platform.

The structure of the paper is the following. In Section II we define the HMM inference problem as the inference problem in a probabilistic graph. Then, in Section III we review the classical sum-product and forward-backward algorithms, introduce the elements and associative operations for parallel operations, and formulate the parallel-scan algorithm on these elements and operators. Next, in Section IV we show that we can apply the parallel-scan concept to the max-product algorithm, which results in a parallel version of the Viterbi algorithm. In Section V we discuss extensions and generalizations of the methodology, and in Section VI we present experimental results for both parallel sum-product and parallel max-product based algorithms. Section VII concludes the article, and additional proofs are provided in Appendix.

II. PROBLEM FORMULATION

Assume that we have T random variables $\mathbf{x} = (x_1, \dots, x_T)$ which correspond to nodes in a probabilistic graph and N potential functions ψ_1, \dots, ψ_N which define the cliques of the graph [33]–[35]. We also assume each variable x_t takes values in set $\mathcal{X} = \{1, \dots, D\}$. Each potential is a function of subset of x_t ’s defined by multi-indices $\alpha_1, \dots, \alpha_T$ with elements $\alpha_t = (\alpha_{t,1}, \dots, \alpha_{t,|\alpha_t|})$. We denote the subsets as \mathbf{x}_{α_t} . The joint distribution of the random variables now has the representation

$$p(\mathbf{x}) = \frac{1}{Z} \prod_{t=1}^T \psi_t(\mathbf{x}_{\alpha_t}), \quad (1)$$

where $Z = \sum_{\mathbf{x}} \prod_{t=1}^T \psi_t(\mathbf{x}_{\alpha_t})$ is the normalization constant which is also called the partition function [33]. Typical inference tasks are now either the computation of all the marginals

$$p(x_k) = \frac{1}{Z} \sum_{\mathbf{x} \setminus x_k} \prod_{t=1}^T \psi_t(\mathbf{x}_{\alpha_t}), \quad (2)$$

where the summation is performed over all the variables except x_k , or the computation of the similar quantity for the maximum:

$$p^*(x_k) = \max_{\mathbf{x} \setminus x_k} \prod_{t=1}^T \psi_t(\mathbf{x}_{\alpha_t}). \quad (3)$$

Let us now consider inference problems in a hidden Markov model (HMM) of the form

$$x_k \sim p(x_k | x_{k-1}), \quad (4a)$$

$$y_k \sim p(y_k | x_k). \quad (4b)$$

Here, we assume that the sequence x_1, \dots, x_T is Markovian with transition probabilities $p(x_k | x_{k-1})$ and the observations y_k are conditionally independent given x_k with likelihoods $p(y_k | x_k)$. Furthermore, we have a prior $x_1 \sim p(x_1)$. We are interested in computing the smoothing posterior distributions of the form $p(x_k | y_1, \dots, y_T)$ for all $k = 1, \dots, T$ as well as in computing the maximum (i.e., Viterbi path) of $p(\mathbf{x})$. These can be computed with sequential algorithms in linear computational time [13], [32], [36]. However, our aim is to improve this computational time by using parallelization in the temporal domain.

We can express the inference problem in (1) by defining

$$\psi_1(x_1) = p(y_1 | x_1) p(x_1), \quad (5a)$$

$$\psi_k(x_{k-1}, x_k) = p(y_k | x_k) p(x_k | x_{k-1}), \quad \text{for } k > 1. \quad (5b)$$

With these definitions the joint distribution (1) takes the form

$$p(\mathbf{x}) = \frac{1}{Z} \psi_1(x_1) \prod_{t=2}^T \psi_t(x_{t-1}, x_t). \quad (6)$$

Thus in this Markovian case, each potential is a function of the neighboring nodes x_{k-1}, x_k , that is, we have $\alpha_k = (k-1, k)$ for $k > 1$ and $\alpha_1 = (1)$.

Typically, the inference task on the HMM is either to compute the marginals $p(x_k | y_1, \dots, y_T)$ or to find the most

probable sequence $x_{1:T}^*$, the Viterbi path. In the potential function formulation, the smoothing distribution is given by (2) and the Viterbi (MAP) path is given by the maximum of (6) or equivalently of (3). Both of these correspond to following kinds of general operations on (6):

$$F(x_k) = \frac{1}{Z} \text{OP}_k \left(\psi_1(x_1) \prod_{t=2}^T \psi_t(x_{t-1}, x_t) \right), k = 1, \dots, T, \quad (7)$$

where, $\text{OP}_k(\cdot)$ is a sequence of operations applied to all elements but x_k , such as $\sum_{\mathbf{x} \setminus x_k}$ or $\max_{\mathbf{x} \setminus x_k}$, resulting in a function of x_k . One way to compute these operations in (7) is to use sum-product or max-product algorithms [37]–[39], for summation and maximization operations, respectively. However, in the following section we show that since sum and max operations are associative, we can use parallel scan algorithms for parallelizing these computations. The same principle would also apply to any other binary associative operations, but here we specifically concentrate on these two operations.

III. PARALLEL SUM-PRODUCT ALGORITHMS FOR HMMs

In this section, we first review the classical sum-product algorithm. Then, we show how to decompose the steps of this algorithm in terms of binary associative operations. We then show how to compute these elements in parallel with $O(\log T)$ span complexity.

A. Classical sum-product algorithm

The sum-product algorithm can be used to find the marginal distribution of all variables in a graph [40], [41]. We first define the forward potential as

$$\psi_{1,k}^f(x_k) = \sum_{x_{1:k-1}} \psi_1(x_1) \prod_{t=2}^k \psi_{t-1,t}(x_{t-1}, x_t) \quad (8)$$

and the backward potential as

$$\psi_{k,T}^b(x_k) = \sum_{x_{k+1:T}} \prod_{t=k}^T \psi_{t,t+1}(x_t, x_{t+1}). \quad (9)$$

We can now express the marginal distribution $p(x_k)$, which corresponds to summation operation in (7), as normalized product of the forward and backward potentials:

$$p(x_k) = \frac{1}{Z_k} \psi_{1,k}^f(x_k) \psi_{k,T}^b(x_k), \quad (10)$$

where $Z_k = \sum_{x_k} \psi_{1,k}^f(x_k) \psi_{k,T}^b(x_k)$. If we want to compute all the marginals $p(x_1), p(x_2), \dots, p(x_T)$, then we need to compute all the terms $\psi_{1,k}^f(x_k)$ and $\psi_{k,T}^b(x_k)$ and combine them. It turns out that we can compute these forward and backward potentials in $O(D^2 T)$ steps using the algorithm in Fig. 2, which is an instance of sum-product algorithm.

It should be noted that the belief propagation algorithm [37], operating on a Bayesian network, corresponds to the sum-product algorithm in a factor graph with similar factorization. The forward algorithm of the HMM model is equivalent to filtering whereas, the backward algorithm corresponds to the backward pass in two-filter smoothing [32].

Require: The potentials $\psi_k(\cdot)$ for $k = 1, \dots, T$.

Ensure: The forward and backward potentials $\psi_{1,k}^f(x_k)$ and $\psi_{k,T}^b(x_k)$ for $k = 1, \dots, T$
// Forward pass:
 $\psi_{1,1}^f(x_1) = \psi_1(x_1)$ ▷ initialization
for $k \leftarrow 2$ **to** T **do** ▷ sequentially
 $\psi_{1,k}^f(x_k) = \sum_{x_{k-1}} \psi_{1,k-1}^f(x_{k-1}) \psi_{k-1,k}(x_{k-1}, x_k)$
end for
// Backward pass:
 $\psi_{T,T}^b(x_T) = 1$ ▷ initialization
for $k \leftarrow T-1$ **to** 1 **do** ▷ sequentially
 $\psi_{k,T}^b(x_k) = \sum_{x_{k+1}} \psi_{k,k+1}(x_k, x_{k+1}) \psi_{k+1,T}^b(x_{k+1})$
end for
return $\psi_{1,k}^f(x_k)$ and $\psi_{k,T}^b(x_k)$ for $k = 1, \dots, T$

Fig. 2. The classical sum-product algorithm for computing the forward and backward potentials.

B. Sum-product algorithm in terms of associative operations

We can formulate sum-product algorithm in a more abstract form by defining a general element $a_{i:k}$ and consider a binary associative operator \otimes such that [25]

$$a_{i:k} = a_{i:j} \otimes a_{j:k}, \text{ for } i < j < k. \quad (11)$$

As is shown in the following, the computation of the forward and backward terms now reduces to computing $a_{0:k}$ and $a_{k:T+1}$.

Definition 1. We define element $a_{i:k}$ recursively as follows. We have

$$\begin{aligned} a_{0:1} &= \psi_1(x_1), \\ a_{k-1:k} &= \psi_k(x_{k-1}, x_k), \\ a_{T:T+1} &= 1. \end{aligned} \quad (12)$$

For notational convenience and to enhance readability, we also define,

$$\begin{aligned} \psi_{0,1}(x_0, x_1) &\triangleq \psi_1(x_1), \\ \psi_{k-1,k}(x_{k-1}, x_k) &\triangleq \psi_k(x_{k-1}, x_k), \\ \psi_{T,T+1}(x_T, x_{T+1}) &\triangleq 1. \end{aligned} \quad (13)$$

Now, given two elements $a_{i:j}$ and $a_{j:k}$, the binary associative operator \otimes for the forward-backward algorithm in HMM for $0 \leq i < j < k$ is

$$a_{i:j} \otimes a_{j:k} = \sum_{x_j} \psi_{i,j}(x_i, x_j) \psi_{j,k}(x_j, x_k), \quad (14)$$

which also implies the following representation for a general element:

$$a_{i:k} = \psi_{i,k}(x_i, x_k). \quad (15)$$

Lemma 1. The operator \otimes is associative.

Proof. The proof of the associative property for forward-backward operator \otimes can be found in Appendix A. \square

Now, we define the theorems to compute the forward-backward algorithm in terms of the associative operations.

Theorem 1. The forward potential is given as

$$a_{0:k} = \psi_{1,k}^f(x_k), \quad k > 0.$$

Proof. Since the operator is associative, it is enough to prove by induction that

$$a_{0:k} = a_{0:1} \otimes a_{1:2} \otimes \cdots \otimes a_{k-2:k-1} \otimes a_{k-1:k} = \psi_{1,k}^f(x_k). \quad (16)$$

Relation (16) holds for $k = 1$ by definition of $a_{0:1}$ in (12). That is $a_{0:1} = \psi_1(x_1)$. Then, we assume that

$$a_{0:k-1} = a_{0:1} \otimes a_{1:2} \otimes \cdots \otimes a_{k-2:k-1} = \psi_{1,k-1}^f(x_{k-1}) \quad (17)$$

holds. We need to prove that Relation (16) holds for k . We start by the binary operation \otimes with $a_{k-1:k}$ in left-hand side of (17)

$$\begin{aligned} & a_{0:k-1} \otimes a_{k-1:k} \\ &= \sum_{x_{k-1}} \psi_{1,k-1}^f(x_{k-1}) \psi_{k-1,k}(x_{k-1}, x_k) \\ &= \sum_{x_{k-1}} \left[\left(\sum_{x_{1:k-2}} \psi_1(x_1) \prod_{t=2}^{k-1} \psi_{t-1,t}(x_{t-1}, x_t) \right) \right. \\ & \quad \left. \times \psi_{k-1,k}(x_{k-1}, x_k) \right] \\ &= \sum_{x_{1:k-1}} \psi_1(x_1) \prod_{t=2}^k \psi_{t-1,t}(x_{t-1}, x_t) \\ &= \psi_{1,k}^f(x_k). \end{aligned}$$

This concludes the proof. \square

Theorem 2. *The backward potential is given as*

$$a_{k:T+1} = \psi_{k,T}^b(x_k), \quad k > 0.$$

Proof. We prove by induction that

$$a_{k:T+1} = a_{k:k+1} \otimes a_{k+1:k+2} \otimes \cdots \otimes a_{T-1:T} \otimes a_{T:T+1} = \psi_{k,T}^b(x_k) \quad (18)$$

holds. Relation (18) holds for $k = T$ by definition of $a_{T:T+1} = 1$ in (12). Then, we assume that

$$a_{k+1:T+1} = a_{k+1:k+2} \otimes a_{k+2:k+3} \otimes \cdots \otimes a_{T:T+1} = \psi_{k+1,T}^b(x_{k+1}) \quad (19)$$

holds. We need to prove that Relation (18) holds for k . We start by the binary operation \otimes with $a_{k:k+1}$ in left-hand side

of (19) to yield

$$\begin{aligned} & a_{k:k+1} \otimes a_{k+1:T+1} \\ &= \sum_{x_{k+1}} \psi_{k,k+1}(x_k, x_{k+1}) \psi_{k+1,T}^b(x_{k+1}) \\ &= \sum_{x_{k+1}} \left[\psi_{k,k+1}(x_k, x_{k+1}) \right. \\ & \quad \left. \times \left(\sum_{x_{k+2:T}} \prod_{t=k+1}^T \psi_{t,t+1}(x_t, x_{t+1}) \right) \right] \\ &= \sum_{x_{k+1:T}} \prod_{t=k}^T \psi_{t,t+1}(x_t, x_{t+1}) \\ &= \psi_{k,T}^b(x_k). \end{aligned}$$

This concludes the proof. \square

Now, we can express the marginal in (10) using $a_{0:k}$ and $a_{k:T+1}$ as

$$p(x_k) = \frac{1}{Z_k} a_{0:k} a_{k:T+1}. \quad (20)$$

In the proofs above we have implicitly used the sum-product algorithm in Fig. 2 to derive the results, which can be done in $O(TD^2)$ steps. However, because the operator is associative, we can reorder the computations by recombining the operations which is the key to parallelization. This is discussed next.

C. Parallelization of the sum-product algorithm

In this section, the aim is to turn the computation of the forward and backward potentials into a parallel operation. One of the fundamental building blocks of parallel algorithms is the prefix-sums operation which can be computed with parallel scan algorithm [24], [25]. This is defined in the following. \square

Definition 2. *For a sequence of T elements (a_1, a_2, \dots, a_T) and a binary associative operator \circ , the all-prefix-sums operation computes the sequence as*

$$(a_1, a_1 \circ a_2, \dots, a_1 \circ a_2 \circ \dots \circ a_T). \quad (21)$$

Similarly to above, we can define reversed prefix-sums as follows.

Definition 3. *For a sequence of T elements (a_1, a_2, \dots, a_T) and a binary associative operator \circ , the reversed all-prefix-sums operation computes the sequence as*

$$(a_1 \circ a_2 \circ \dots \circ a_T, \dots, a_{T-1} \circ a_T, a_T). \quad (22)$$

It turns out that the all-prefix-sums above can be computed with the parallel-scan algorithm [24], [25] in span $O(\log T)$ time. A pseudocode for the algorithm is shown in Fig. 3. The algorithm computes the non-reversed all-prefix-sums only, but by reversing the input before and after the call (and reversing the operation inside the algorithm), it can also be used to compute the reversed prefix sums.

Require: The elements a_k for $k = 1, \dots, T$ and operator \otimes .
Ensure: The prefix sums in a_k for $k = 1, \dots, T$

```

// Save the input:
for  $i \leftarrow 1$  to  $T$  do                                ▷ Compute in parallel
     $b_i \leftarrow a_i$ 
end for
// Up sweep:
for  $d \leftarrow 0$  to  $\log_2 T - 1$  do
    for  $i \leftarrow 0$  to  $T - 1$  by  $2^{d+1}$  do ▷ Compute in parallel
         $j \leftarrow i + 2^d$ 
         $k \leftarrow i + 2^{d+1}$ 
         $a_k \leftarrow a_j \otimes a_k$ 
    end for
end for
 $a_n \leftarrow 0$ 
// Down sweep:
for  $d \leftarrow \log_2 T - 1$  to  $0$  do
    for  $i \leftarrow 0$  to  $T - 1$  by  $2^{d+1}$  do ▷ Compute in parallel
         $j \leftarrow i + 2^d$ 
         $k \leftarrow i + 2^{d+1}$ 
         $t \leftarrow a_j$ 
         $a_j \leftarrow a_k$ 
         $a_k \leftarrow a_k \otimes t$ 
    end for
end for
// Final pass:
for  $i \leftarrow 1$  to  $T$  do                                ▷ Compute in parallel
     $a_i \leftarrow a_i \otimes b_i$ 
end for
return  $a_{1:T}$ 

```

Fig. 3. Parallel-scan algorithm for in-place transformation of the sequence (a_i) into its all-prefix-sums in $O(\log T)$ span-complexity. Note that the algorithm in this form assumes that T is a power of 2, but it can easily be generalized to an arbitrary T .

We can now notice that computation of the forward potentials in fact corresponds to computation of prefix sums for the associative operation \otimes and elements $a_{i:i+1}$:

$$\begin{aligned}
 a_{0:1} &= \psi_{1,1}^f(x_1) \\
 a_{0:2} &= a_{0:1} \otimes a_{1:2} = \psi_{1,2}^f(x_2), \\
 &\vdots \\
 a_{0:T} &= a_{0:1} \otimes \dots \otimes a_{T-1:T} = \psi_{1,T}^f(x_T).
 \end{aligned} \tag{23}$$

Similarly, computing the backward potentials which correspond to elements $a_{k,T}$ can be seen as reversed prefix sums.

Therefore, we can use the parallel-scan algorithm to compute the forward and backward potentials along with the marginal distributions (20) in parallel using algorithm in Fig. 4.

As all the steps in algorithm in Fig. 4 are either fully parallelizable, or are parallelizable by the parallel-scan algorithm, then span and work complexities can be summarized as follows.

Proposition 1. *The parallel sum-product algorithm in Fig. 4 has span complexity $O(\log T)$ and work complexity $O(T)$.*

Require: The potentials $\psi_k(\cdot)$, $k = 1, \dots, T$ and operator \otimes .
Ensure: The marginals $p(x_k)$ for $k = 1, \dots, T$.

```

for  $k \leftarrow 1$  to  $T$  do                                ▷ In parallel
    Initialize  $a_{k-1:k}$ 
end for
Run parallel-scan to get  $a_{0:k} = \psi_{1,k}^f(x_k)$ ,  $k = 1, \dots, T$ .
for  $k \leftarrow 1$  to  $T$  do                                ▷ In parallel
    Initialize  $a_{k:k+1}$ 
end for
Run reversed parallel-scan to get  $a_{k:T+1} = \psi_{k,T}^b(x_k)$ ,  $k = 1, \dots, T$ .
for  $k \leftarrow 1$  to  $T$  do                                ▷ In parallel
    Compute marginal  $p(x_k)$  using (20)
end for
return All marginals  $p(x_k)$ ,  $k = 1, \dots, T$  ▷ In parallel

```

Fig. 4. Parallel sum-product algorithm.

Proof. The initializations for the elements for both the forward and backward passes as well as the marginal computations are fully parallelizable and hence have span complexities $O(1)$ and work complexities $O(T)$. The parallel-scan algorithm passes have span complexities $O(\log T)$ and work complexities $O(T)$. Therefore the total span complexity is $O(\log T)$ and the total work complexity is $O(T)$. \square

It is useful to remark that the computational complexity also depends on the dimensionality D . However, it depends on the details how much we can parallelize inside the initializations and operator applications, which is what determines the dependence of the span complexity on D .

IV. PARALLEL VITERBI AND MAX-PRODUCT ALGORITHMS

In this section, we first review the classical Viterbi algorithm and its max-product version. Then, we decompose the elements of the latter algorithm in terms of binary associative operations which is a similar operation as sum-product algorithm but for “max” instead of “sum” operation. Finally, we show how to compute these elements in parallel with $O(\log T)$ span complexity.

Please note that in this paper, we assume that the most probable (MAP) path is unique for simplicity of exposition. However, the results can be easily extended to account for multiple solutions.

A. Classical Viterbi algorithm

In HMM literature, the *Viterbi algorithm* is a classical algorithm based on dynamic programming principle that computes the most likely sequence of states [2], [13], [42], that is, *maximum-a-posteriori* (MAP) estimate of the hidden states. We aim to compute the estimate $x_{1:T}^*$ by maximizing the posterior distribution

$$p(x_{1:T} | y_{1:T}) = \frac{p(y_{1:T}, x_{1:T})}{p(y_{1:T})} \propto p(y_{1:T}, x_{1:T}) \tag{24}$$

which is equivalent to maximizing the joint probability distribution

$$p(y_{1:T}, x_{1:T}) = p(x_1) p(y_1 | x_1) \prod_{t=2}^T p(y_t | x_t) p(x_t | x_{t-1}), \quad (25)$$

that is,

$$x_{1:T}^* = \arg \max_{x_{1:T}} p(y_{1:T}, x_{1:T}). \quad (26)$$

In terms of potentials, this is also equivalent to maximization of (6).

The classical Viterbi algorithm [2], [13] operates as follows. Assume that we have $V_{k-1}(x_{k-1})$ which is the probability of the maximum probability path $x_{1:k-1}^*$ which ends at x_{k-1} . Then the maximum probability of a path ending at $V_k(x_k)$ and the corresponding optimal state x_{k-1}^* (as function of x_k hence denoted as $u_{k-1}(x_k)$) are given by

$$\begin{aligned} V_k(x_k) &= \max_{x_{k-1}} [p(y_k | x_k) p(x_k | x_{k-1}) V_{k-1}(x_{k-1})], \\ u_{k-1}(x_k) &= \arg \max_{x_{k-1}} [p(y_k | x_k) p(x_k | x_{k-1}) V_{k-1}(x_{k-1})], \end{aligned} \quad (27)$$

with initial condition

$$V_1(x_1) = p(x_1) p(y_1 | x_1). \quad (28)$$

At the final step we then just take

$$x_T^* = \max_{x_T} V_T(x_T) \quad (29)$$

and then we just compute backwards

$$x_{k-1}^* = u_{k-1}(x_k^*). \quad (30)$$

In terms of potentials the pseudocode for Viterbi algorithm can be written as in Fig. 5. As the computational complexity of the forward pass is $O(D^2T)$ and backward pass is $O(T)$, therefore, the total computational complexity of the Viterbi algorithm is $O(D^2T)$.

Require: The potentials $\psi_k(\cdot)$ for $k = 1, \dots, T$

Ensure: The Viterbi path $x_{1:T}^*$

// Forward pass:

$$V_1(x_1) = \psi_1(x_1)$$

for $k \leftarrow 2$ **to** T **do** ▷ sequentially

$$V_k(x_k) = \max_{x_{k-1}} [\psi_k(x_{k-1}, x_k) V_{k-1}(x_{k-1})]$$

$$u_{k-1}(x_k) = \arg \max_{x_{k-1}} [\psi_k(x_{k-1}, x_k) V_{k-1}(x_{k-1})]$$

end for

// Backward pass:

$$x_T^* = \arg \max_{x_T} V_T(x_T)$$

for $k \leftarrow T$ **to** 2 **do**

$$x_{k-1}^* = u_{k-1}(x_k^*)$$

end for

return $x_{1:T}^*$

Fig. 5. The classical Viterbi algorithm.

B. Path-based parallelization

In order to design a parallel version of the Viterbi algorithm, we first need to find an element \tilde{a} and the binary associative operator \vee for the Viterbi algorithm.

Definition 4. For two elements

$$\tilde{a}_{i:j} = \begin{pmatrix} A_{i:j}(x_i, x_j) \\ \hat{X}_{i:j}(x_i, x_j) \end{pmatrix}, \quad \tilde{a}_{j:k} = \begin{pmatrix} A_{j:k}(x_j, x_k) \\ \hat{X}_{j:k}(x_j, x_k) \end{pmatrix}, \quad (31)$$

the binary associative operator \vee for the maximum a posteriori (MAP) path in HMM is defined as

$$\tilde{a}_{i:k} = \tilde{a}_{i:j} \vee \tilde{a}_{j:k}, \quad (32)$$

where

$$\begin{aligned} \tilde{a}_{i:k} &= \begin{pmatrix} A_{i:k}(x_i, x_k) \\ \hat{X}_{i:k}(x_i, x_k) \end{pmatrix} \\ &= \begin{pmatrix} \max_{x_j} A_{i:j}(x_i, x_j) A_{j:k}(x_j, x_k) \\ \left(\hat{X}_{i:j}(x_i, \hat{x}_j(x_i, x_k)), \hat{x}_j(x_i, x_k), \hat{X}_{j:k}(\hat{x}_j(x_i, x_k), x_k) \right) \end{pmatrix} \end{aligned} \quad (33)$$

and

$$\hat{x}_j(x_i, x_k) = \arg \max_{x_j} A_{i:j}(x_i, x_j) A_{j:k}(x_j, x_k) \quad (34)$$

with

$$\begin{aligned} A_{k-1:k}(x_{k-1}, x_k) &= \psi_{k-1,k}(x_{k-1}, x_k), \\ \hat{X}_{k-1:k}(x_{k-1}, x_k) &= \emptyset, \\ A_{0:1}(\cdot, x_1) &= \psi_1(x_1), \\ \hat{X}_{0:1}(\cdot, x_1) &= \emptyset. \end{aligned} \quad (35)$$

Lemma 2. The operator \vee is associative.

Proof. The proof of associative property of the operator \vee can be found in Appendix B. \square

Theorem 3. We have

$$A_{i:j}(x_i, x_j) = \max_{x_{i+1:j-1}} \prod_{k=i+1}^j \psi_{k-1,k}(x_{k-1}, x_k), \quad (36)$$

$$\hat{X}_{i:j}(x_i, x_j) = \arg \max_{x_{i+1:j-1}} \prod_{k=i+1}^j \psi_{k-1,k}(x_{k-1}, x_k),$$

where $A_{i:j}$ corresponds to the maximum probability of MAP path starting from x_i and ending at x_j , and $\hat{X}_{i:j}$ represents the sequence of the corresponding paths.

Proof. The proof is provided in Appendix C. \square

By putting $i = 0$ and $j = T + 1$ in Theorem 3 above we now obtain the following result.

Corollary 1. We have

$$\tilde{a}_{0:T+1} = \begin{pmatrix} \psi_1(x_1^*) \prod_{t=2}^T \psi_{t-1,t}(x_{t-1}^*, x_t^*) \\ x_{1:T}^* \end{pmatrix},$$

where $x_{1:T}^*$ is the MAP estimate given by (26).

It would now be possible to form a parallel algorithm for the elements $\tilde{a}_{i:j}$ with the associative operator \vee by leveraging

the parallel-scan algorithm for computing the quantity in Corollary 1. However, each element $\tilde{a}_{i:j}$ contains a path of length $j - i - 2$ for each state pair and therefore, the memory requirements to store the state sequences are high. Thus, in the next section, we propose an alternative approach with lower memory requirements.

C. Max-product formulation

Until now, we have used the Viterbi algorithm in forward direction. However, the MAP path can also be computed by using the max-product algorithm (see cf. [33]). Let us denote by $\tilde{\psi}_k^f(x_k)$ the maximum probability of the optimal path ending at x_k and the maximum probability of starting at x_k as $\tilde{\psi}_k^b(x_k)$ which are thus given as

$$\begin{aligned}\tilde{\psi}_k^f(x_k) &= A_{0:k}(x_0, x_k), \\ \tilde{\psi}_k^b(x_k) &= A_{k:T+1}(x_k, x_{T+1}),\end{aligned}\quad (37)$$

where the dependence on x_0 and x_{T+1} is only notational (cf. (13)). From Definition 4 we now get the following recursions for these quantities.

Lemma 3. *The maximum forward and backward probabilities admit the recursions*

$$\begin{aligned}\tilde{\psi}_k^f(x_k) &= \max_{x_{k-1}} \psi_{k-1:k}(x_{k-1}, x_k) \tilde{\psi}_{k-1}^f(x_{k-1}), \\ \tilde{\psi}_k^b(x_k) &= \max_{x_{k+1}} \psi_{k:k+1}(x_k, x_{k+1}) \tilde{\psi}_{k+1}^b(x_{k+1}),\end{aligned}\quad (38)$$

with initial conditions $\tilde{\psi}_1^f(x_1) = \psi_1(x_1)$ and $\tilde{\psi}_T^b(x_T) = 1$.

It then turns out that the optimal states can be computed by maximizing the product $\tilde{\psi}_k^f(x_k) \tilde{\psi}_k^b(x_k)$. This is summarized in the following theorem.

Theorem 4. *Given the maximum forward potentials $\tilde{\psi}_k^f(x_k)$ and the maximum backward potentials $\tilde{\psi}_k^b(x_k)$, the global optimum is determined by*

$$x_k^* = \arg \max_{x_k} \tilde{\psi}_k^f(x_k) \tilde{\psi}_k^b(x_k) \quad (39)$$

for $k = 1, \dots, T$.

Proof. The proof can be found in Appendix D. \square

Theorem 4 follows from the generalized MAP estimates for an arbitrary graph discussed in [33, ch. 13]. However, we compute the elements of these forward and backward potentials in parallel.

Let us now define element $\bar{a}_{i:j}$ to consist of the upper part of $\tilde{a}_{i:j}$ where the path is left out. These elements can be computed without actually storing the paths $x_{i:j}^*$ which provides a computational advantage.

Definition 5. *For two elements $\bar{a}_{i:j} = A_{i:j}(x_i, x_j)$ and $\bar{a}_{j:k} = A_{j:k}(x_j, x_k)$, the binary operator \vee can be defined as*

$$\bar{a}_{i:k} = \bar{a}_{i:j} \vee \bar{a}_{j:k}, \quad (40)$$

where

$$\bar{a}_{i:k} = \max_{x_j} A_{i:j}(x_i, x_j) A_{j:k}(x_j, x_k). \quad (41)$$

The element $\bar{a}_{i:j}$ and the operator also inherit the associative property of the element $\tilde{a}_{i:j}$, and therefore, we also have $\bar{a}_{i:k} = A_{i:k}(x_i, x_k)$.

We also define the operator \vee similarly for the elements $\bar{a}_{i:j}$ as for $\tilde{a}_{i:j}$. We can now compute the maximum forward and backward potentials in terms of these associative operators and elements, which is summarized in the following.

Proposition 2. *The maximum forward potential can also be computed as*

$$\bar{a}_{0:k} = \tilde{\psi}_k^f(x_k), \quad k > 0.$$

Proof. This follows from Theorem 3. \square

Proposition 3. *The maximum backward potential can be computed as*

$$\bar{a}_{k:T+1} = \tilde{\psi}_k^b(x_k), \quad k > 0.$$

Proof. This follows from Theorem 3. \square

Similar to the sum-product algorithm in Section III-C, we can now parallelize the max-product algorithm. The steps are summarized in the algorithm in Fig. 6. The span and work complexities of the algorithm are summarized in the following proposition.

Require: The potentials $\psi_k(\cdot)$, $k = 1, \dots, T$ and operator \vee .
Ensure: The Viterbi path $x_{1:T}^*$.

```

for  $k \leftarrow 1$  to  $T$  do ▷ In parallel
  Initialize  $\bar{a}_{k-1:k}$ 
end for
Run parallel-scan to get  $\bar{a}_{0:k} = \tilde{\psi}_{1,k}^f(x_k)$ ,  $k = 1, \dots, T$ .
for  $k \leftarrow 1$  to  $T$  do ▷ In parallel
  Initialize  $\bar{a}_{k:k+1}$ 
end for
Run reversed parallel-scan to get  $\bar{a}_{k:T+1} = \tilde{\psi}_{k,T}^b(x_k)$ ,  $k = 1, \dots, T$ .
for  $k \leftarrow 1$  to  $T$  do ▷ In parallel
  Compute the optimal state  $x_k^*$  using (39)
end for
return  $x_{1:T}^*$  ▷ In parallel

```

Fig. 6. Parallel max-product (Viterbi) algorithm.

Proposition 4. *The span complexity of the parallel max-product algorithm in Fig. 6 is $O(\log T)$ and the work complexity is $O(T)$.*

Proof. The initializations and final state combinations have the span complexity $O(1)$ and work complexity $O(T)$, and the scans have the span complexity $O(\log T)$ and work complexity $O(T)$. Hence the result follows. \square

V. EXTENSIONS

In this section, we discuss extensions of the parallel-scan framework.

A. Generic associative operations

We defined the parallel-scan framework in terms of sum-products and max-products for hidden Markov models (HMMs). We can easily extend this proposed framework for operations of the form (7) for arbitrary associative operators. In particular, we can also consider continuous-state Markov processes in which case the operator becomes integration. In this case we get similar algorithms to ones described in [30] except that the smoother will be a two-filter smoother instead of the Rauch–Tung–Striebel smoother as in [30]. In particular, for linear Gaussian systems we get a parallel version of the two-filter Kalman smoother.

B. Block-wise operations

In this article, we have restricted our consideration to pairwise Markovian elements. That is, we assign each single observation and state to a single element. However, it is possible to perform binary association operations in parallel on a block of observations. We can define a block of observations and states to elements of the parallel framework. The processing of elements in parallel with a block of length l is already been shown in [30]. The practical advantage is that we can more easily distribute the computations where the resources are limited and still achieving the optimal speed from parallelization.

C. Parameter estimation

The final task of HMM inference is learning the model parameters. One possible solution is to use *Baum-Welch algorithm* (BWA) [43], which is a special case of *expectation-maximization* (EM) algorithm [44]. In expectation step, BWA uses the forward-backward algorithm which we have shown to be computed in parallel.

VI. EXPERIMENTAL RESULTS

For our experiment, we consider the Gilbert–Elliott (GE) channel model [2], which is a classical model used in transmission of signals in digital communication channels. The model describes the burst error patterns in communication channels and simulates the error performance of the communication link. This model consists of two hidden Markov states b_k and s_k , where the b_k represents the binary input signal to be transmitted and s_k represents the channel regime binary signal. It is assumed that the input signal b_k may be flipped by an independent error which can be modeled as $y_k = b_k \oplus v_k$. Here, y_k is the measurement signal which is observable, v_k is a Bernoulli sequence and \oplus is the exclusive-or operation. The exclusive-or operation ensures that $y_k = b_k$, if $p(v_k) = 0$, otherwise $y_k \neq b_k$ and an error has occurred.

The regime input signal s_k is modeled as a two-state Markov chain that represents high and low error conditions of the channel. That is, if an error occurs ($p(v_k) = 1$), the probability of error has either a small value (q_0) or a larger value (q_1). Moreover, we represent the probability of transition from high error state ($s_{k-1} = 1$) to low error state ($s_k = 0$) as p_0 . Similarly, we present the probability of transition from

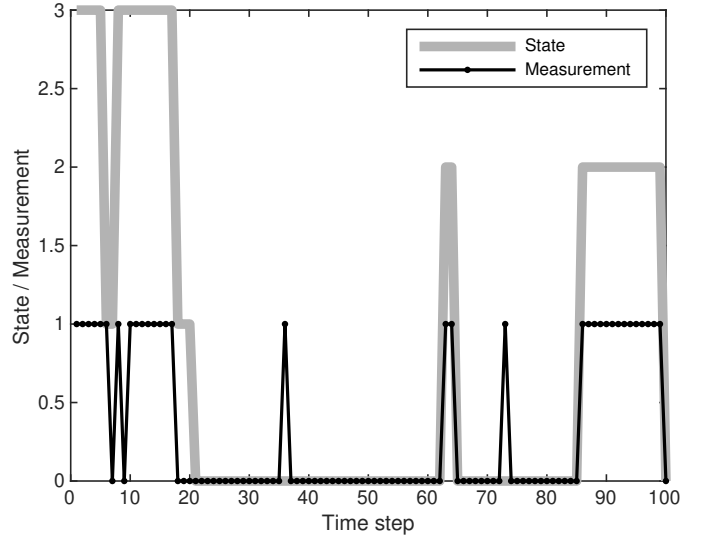


Fig. 7. An example of states and measurements from the Gilbert–Elliott hidden Markov model with the number of time steps $T = 100$.

low error state ($s_{k-1} = 0$) to high error state ($s_k = 1$) as p_1 . We also denote the state switch probability of b_k as p_2 .

In order to recover the hidden states, we use the joint model $x_k = (s_k, b_k)$ which is a 4-state Markov chain consisting of the states $\{(0, 0), (0, 1), (1, 0), (1, 1)\}$. These states are encoded as $\{0, 1, 2, 3\}$. The transition matrix Π and the observation model O , which encode the information in $p(x_k | x_{k-1})$ and $p(y_k | x_k)$, respectively, are given in (42). An example of the states and the corresponding measurements from the GE model is shown in Fig. 7.

To evaluate the performance of our proposed methods, we simulated the states and measurements with varying lengths of time series ranging from $T = 10^2$ to $T = 10^5$ and averaged the run times (10 repetitions for sequential methods and 100 for parallel ones). In the experimental setup, we used the open-source TensorFlow 2.4 software library [45]. The library natively implements the vectorization and associative scan primitives that can be used to implement the methodology for both CPUs and GPUs. We ran the sequential and parallel Bayesian smoothers [32] (BS-Seq, BS-Par), sequential and parallel sum-product based smoothers (SP-Seq, SP-Par) from Section III, and, sequential and parallel max-product based MAP estimators (MP-Seq, MP-Par) from Section IV on both CPU and GPU. We also ran the classical Viterbi algorithm (see Fig. 5) for comparison. The experiment was carried both on a CPU, AMD Ryzen™ Threadripper™ 3960X with 24 Cores and 3.8 GHz, and a GPU, NVIDIA® Ampere® GeForce RTX 3090 (GA102) with 10496 cores.

The average run times are shown in Figs. 8 and 9. It is clear that the parallel algorithms are computationally faster than the sequential versions both on CPU and GPU. Although the difference is much more pronounced on GPU, even on CPU, we can see a benefit of parallelization. Nevertheless, the number of computational cores is orders of magnitude smaller than in the GPU (24 vs. 10496 cores). Among the compared methods, the max-product-based parallel method is the fastest, sum-product-based parallel method is the second,

$$\Pi = \begin{pmatrix} (1-p_0)(1-p_2) & p_0(1-p_2) & (1-p_0)p_2 & p_0p_2 \\ p_1(1-p_2) & (1-p_1)(1-p_2) & p_1p_2 & (1-p_1)p_2 \\ (1-p_0)p_2 & p_0p_2 & (1-p_0)(1-p_2) & p_0(1-p_2) \\ p_1p_2 & (1-p_1)p_2 & p_1(1-p_2) & (1-p_1)(1-p_2) \end{pmatrix}, \quad O = \begin{pmatrix} (1-q_0) & q_0 \\ (1-q_1) & q_1 \\ q_0 & (1-q_0) \\ q_1 & (1-q_1) \end{pmatrix}. \quad (42)$$

Here,

$$\Pi = p(x_k | x_{k-1})$$

and

$$O = p(y_k | x_k).$$

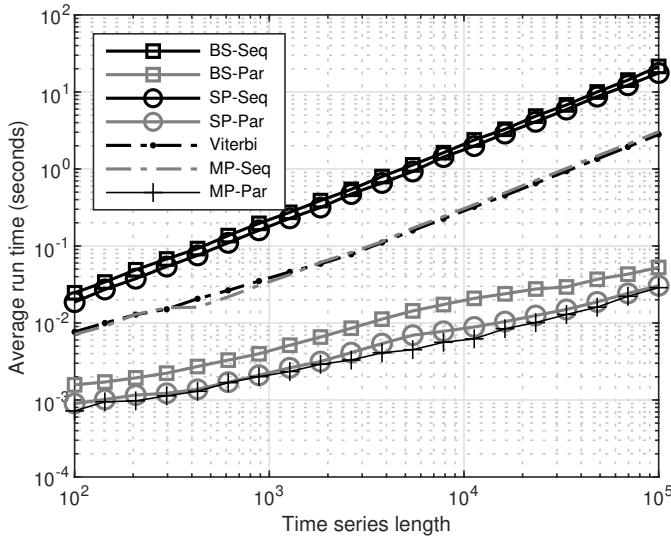


Fig. 8. The average computation times on CPU for sequential and parallel Bayesian smoothers (BS-Seq, BS-Par), sequential and parallel sum-product algorithms (SP-Seq, SP-Par), sequential and parallel max-product algorithms (MP-Seq, MP-Par), and the classical Viterbi algorithm (Viterbi).

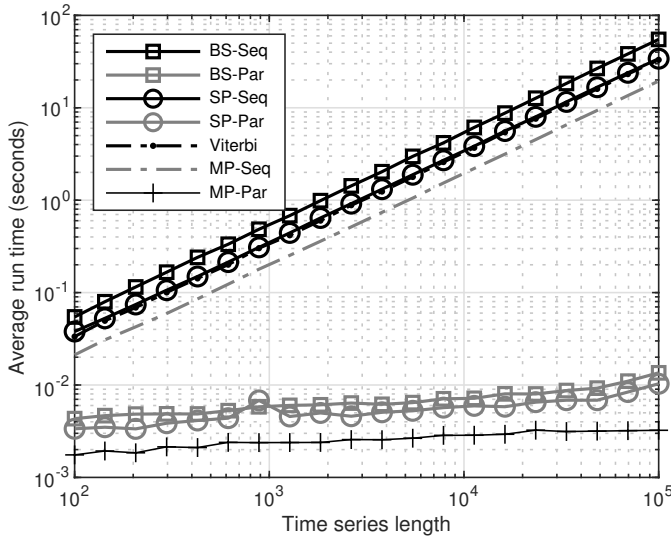


Fig. 9. The average computation times on GPU for sequential and parallel Bayesian smoothers (BS-Seq, BS-Par), sequential and parallel sum-product algorithms (SP-Seq, SP-Par), sequential and parallel max-product algorithms (MP-Seq, MP-Par), and the classical Viterbi algorithm (Viterbi).

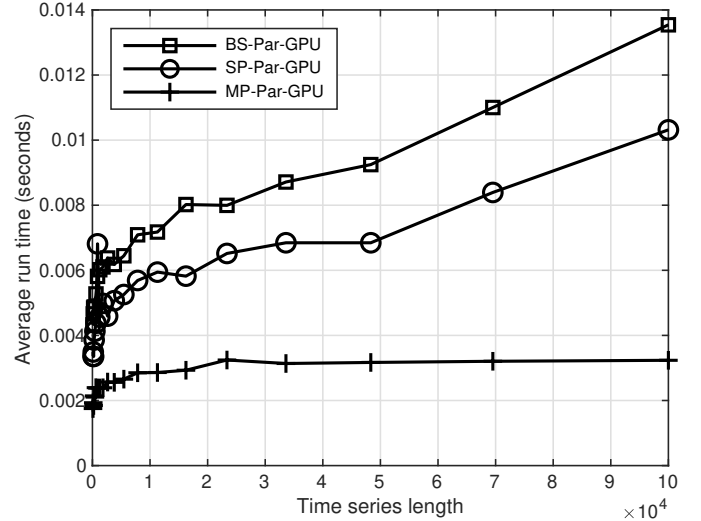


Fig. 10. The average computation times on GPU for parallel Bayesian smoothers (BS-Par-GPU), parallel sum-product algorithms (SP-Par-GPU), and parallel max-product algorithms (MP-Par-GPU).

and the parallel Bayesian smoother is the third, on both CPU and GPU. A similar order can be seen among the sequential method results and the classical Viterbi is placed between the other sequential methods.

The average run times of the parallel methods on GPU (on a linear scale) are separately shown in Fig. 10. From the figure it can be seen that the computational times initially grow logarithmically as is predicted by the theory and then, for the Bayesian smoother and sum-product method retain back to linear when the time series length becomes longer than $\sim 5 \times 10^4$. However, the max-product method remains sub-linear even beyond 10^5 , which is likely due to less computational operations needed.

Finally, Fig. 11 shows the ratio of the average run times of the sequential methods and the corresponding parallel methods on GPU. It can be seen that with time series length of $\sim 5 \times 10^4$, the speed-up is already between 2000–3000 and with time series of length 10^5 , the speed-up in the max-product method is ~ 6000 . On the other hand, with the Bayesian smoother and sum-product methods it is ~ 3000 –4000.

VII. CONCLUSION

In this paper, we have proposed a parallel formulation of HMM inference. We have considered the computation of both

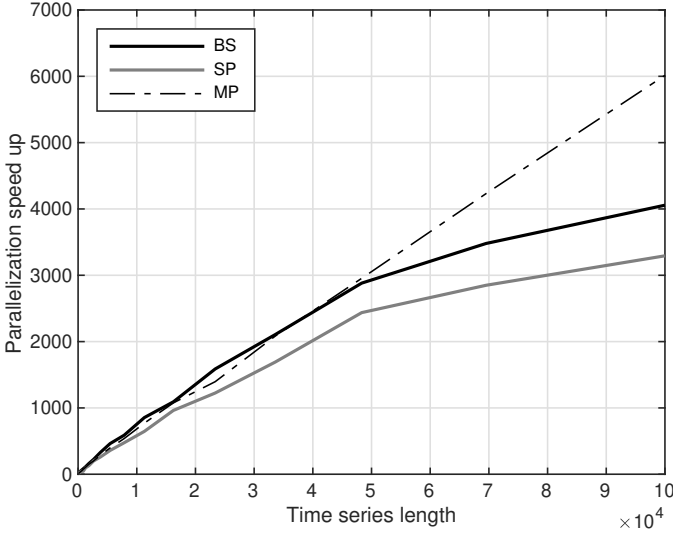


Fig. 11. The ratio of the average run times of the sequential methods (BS) and the corresponding parallel methods (SP, MP) on GPU.

the marginal smoothing distributions as well as the MAP (Viterbi) paths. The proposed formulation enables the efficient parallel computation of the HMM inference by reducing the time complexity from linear to logarithmic scales. The algorithms are based on reformulating the HMM inference problems in terms of associative operations which can be parallelized using the parallel-scan algorithm. We also showed the practical advantage of our proposed methods with experiments in multi-core CPU and GPU.

APPENDIX

A. Proof of Lemma 1

In this section, we prove the associative property of the operator \otimes stated in Lemma 1. For this, we need to prove that for three general elements $a_{i:j}$, $a_{j:k}$, $a_{k:l}$, the following relation holds

$$(a_{i:j} \otimes a_{j:k}) \otimes a_{k:l} = a_{i:j} \otimes (a_{j:k} \otimes a_{k:l}), \quad (43)$$

where, $0 \leq i < j < k < l$.

We proceed to perform the calculations on left-hand side of (43) to check that they yield the same result as on right-hand side:

$$\begin{aligned} & (a_{i:j} \otimes a_{j:k}) \otimes a_{k:l} \\ &= \sum_{x_k} \left(\sum_{x_j} \psi_{i,j}(x_i, x_j) \psi_{j,k}(x_j, x_k) \right) \psi_{k,l}(x_k, x_l) \\ &= \sum_{x_j, x_k} \psi_{i,j}(x_i, x_j) \psi_{j,k}(x_j, x_k) \psi_{k,l}(x_k, x_l) \\ &= \sum_{x_j} \psi_{i,j}(x_i, x_j) \left(\sum_{x_k} \psi_{j,k}(x_j, x_k) \psi_{k,l}(x_k, x_l) \right) \\ &= a_{i:j} \otimes (a_{j:k} \otimes a_{k:l}), \end{aligned}$$

which gives the result.

B. Proof of Lemma 2

In this section, we prove the associative property of the operator \vee as stated in Lemma 2. We need to prove that for three general elements $\tilde{a}_{i:j}$, $\tilde{a}_{j:k}$, $\tilde{a}_{k:l}$, the following relation holds

$$(\tilde{a}_{i:j} \vee \tilde{a}_{j:k}) \vee \tilde{a}_{k:l} = \tilde{a}_{i:j} \vee (\tilde{a}_{j:k} \vee \tilde{a}_{k:l}), \quad (44)$$

where, $0 \leq i < j < k < l$.

From Definition 4, we can write

$$\tilde{a}_{i:j} \vee \tilde{a}_{j:k} = \left(A_{i:k}(x_i, x_k) \right), \quad (45)$$

where

$$A_{i:k}(x_i, x_k) = \max_{x_j} A_{i:j}(x_i, x_j) A_{j:k}(x_j, x_k), \quad (46a)$$

$$\hat{X}_{i:k}(x_i, x_k) = \left(\hat{X}_{i:j}(x_i, \hat{x}_j(x_i, x_j)), \hat{x}_j(x_i, x_j), \hat{X}_{j:k}(\hat{x}_j(x_i, x_j), x_k) \right), \quad (46b)$$

and

$$\hat{x}_j(x_i, x_j) = \arg \max_{x_j} A_{i:j}(x_i, x_j) A_{j:k}(x_j, x_k). \quad (47)$$

Now, combining the maximum probability of MAP path for the element $\tilde{a}_{k:l}$, we can write (46a) as

$$\begin{aligned} A_{i:l}(x_i, x_l) &= \max_{x_k} A_{i:k}(x_i, x_k) A_{k:l}(x_k, x_l) \\ &= \max_{x_k} \left[\left\{ \max_{x_j} A_{i:j}(x_i, x_j) A_{j:k}(x_j, x_k) \right\} \right. \\ &\quad \left. \times A_{k:l}(x_k, x_l) \right] \\ &= \max_{x_j} \left[A_{i:j}(x_i, x_j) \right. \\ &\quad \left. \times \left\{ \max_{x_k} A_{j:k}(x_j, x_k) A_{k:l}(x_k, x_l) \right\} \right] \\ &= \max_{x_j} A_{i:j}(x_i, x_j) A_{j:l}(x_j, x_l). \end{aligned} \quad (48)$$

Now, combining the MAP path of the element $\tilde{a}_{k:l}$, we can write (46b) as

$$\begin{aligned} \hat{X}_{i:l}(x_i, x_l) &= \arg \max_{x_k} A_{i:k}(x_i, x_k) A_{k:l}(x_k, x_l) \\ &= \arg \max_{x_k} \left[\left\{ \arg \max_{x_j} A_{i:j}(x_i, x_j) A_{j:k}(x_j, x_k) \right\} \right. \\ &\quad \left. \times A_{k:l}(x_k, x_l) \right] \\ &= \arg \max_{x_j} \left[A_{i:j}(x_i, x_j) \right. \\ &\quad \left. \times \left\{ \arg \max_{x_k} A_{j:k}(x_j, x_k) A_{k:l}(x_k, x_l) \right\} \right] \\ &= \arg \max_{x_j} A_{i:j}(x_i, x_j) A_{j:l}(x_j, x_l). \end{aligned} \quad (49)$$

From (48) and (49), it follows that the operator \vee is associative.

C. Proof of Theorem 3

In this section, we prove Theorem 3 by induction. We first note that the theorem is true for $i = k$ and $j = k + 1$. Furthermore, if the assertion is true for $i + 1 < j$, we proceed to show that it holds for i . By using (33) we get

$$\begin{aligned} & A_{i:j}(x_i, x_j) \\ &= \max_{x_{i+1}} A_{i:i+1}(x_i, x_{i+1}) A_{i+1:j}(x_{i+1}, x_j) \\ &= \max_{x_{i+1}} \psi_{i,i+1}(x_i, x_{i+1}) \max_{x_{i+2:j-1}} \prod_{t=i+2}^j \psi_{t-1,t}(x_{t-1}, x_t) \quad (50) \\ &= \max_{x_{i+1:j-1}} \prod_{t=i+1}^j \psi_{t-1,t}(x_{t-1}, x_t). \end{aligned}$$

We similarly get

$$\begin{aligned} & \hat{X}_{i:j}(x_i, x_j) \\ &= \left(\hat{X}_{i:i+1}(x_i, \hat{x}_{i+1}(x_i, x_j)), \hat{x}_{i+1}(x_i, x_j), \right. \\ & \quad \left. \hat{X}_{i+1:j}(\hat{x}_{i+1}(x_i, x_j), x_j) \right) \\ &= \left(\hat{x}_{i+1}(x_i, x_j), \hat{X}_{i+1:j}(\hat{x}_{i+1}(x_i, x_j), x_j) \right) \\ &= \left(\arg \max_{x_{i+1}} \psi_{i,i+1}(x_i, x_{i+1}) \max_{x_{i+2:j-1}} \prod_{t=i+2}^j \psi_{t-1,t}(x_{t-1}, x_t), \right. \\ & \quad \left. \max_{x_{i+1}} \arg \max_{x_{i+2:j-1}} \prod_{t=i+2}^j \psi_{t-1,t}(x_{t-1}, x_t) \right) \\ &= \arg \max_{x_{i+1:j-1}} \prod_{t=i+1}^j \psi_{t-1,t}(x_{t-1}, x_t), \quad (51) \end{aligned}$$

which concludes the proof.

D. Proof of Theorem 4

In this section, we prove Theorem 4. That is, given the maximum forward probability $\tilde{\psi}_k^f(x_k)$ of path ending at x_k , and the maximum backward probability $\tilde{\psi}_k^b(x_k)$ of path starting at x_k , the global optimum is given by (39).

Due to associative property of the operator, we can now write

$$\tilde{a}_{0:T+1} = \tilde{a}_{0:k} \vee \tilde{a}_{k:T+1} = \left(\psi_1(x_1^*) \prod_{t=2}^T \psi_t(x_{t-1}^*, x_t^*) \right)_{x_1^*:T} \quad (52)$$

which is given by

$$\begin{aligned} & \tilde{a}_{0:k} \vee \tilde{a}_{k:T+1} \\ &= \left(\max_{x_k} A_{0:k}(x_0, x_k) A_{k:T+1}(x_k, x_{T+1}) \right. \\ & \quad \left(\hat{X}_{0:k}(x_0, \hat{x}_k(x_0, x_{T+1})), \hat{x}_k(x_0, x_{T+1}), \right. \\ & \quad \left. \hat{X}_{k:T+1}(\hat{x}_k(x_0, x_{T+1}), x_{T+1}) \right) \quad (53) \end{aligned}$$

where actually the dependence on x_0 and x_{T+1} is only notational and the term

$$\begin{aligned} & \hat{x}_k(x_0, x_{T+1}) \\ &= \arg \max_{x_k} A_{0:k}(x_0, x_k) A_{k:T+1}(x_k, x_{T+1}) \quad (54) \\ &= \arg \max_{x_k} \tilde{\psi}^f(x_k) \tilde{\psi}^b(x_k) \end{aligned}$$

has to be the k th element on the optimal path in order to match the right hand side of (52).

ACKNOWLEDGMENT

The authors would like to thank Academy of Finland for funding. The authors would also like to thank Adrien Corenflos for helping with the experiments.

REFERENCES

- [1] L. R. Rabiner, "A tutorial on hidden Markov models and selected applications in speech recognition," *Proceedings of the IEEE*, vol. 77, no. 2, pp. 257–286, 1989.
- [2] O. Cappé, E. Moulines, and T. Rydén, *Inference in hidden Markov models*. Springer, 2006.
- [3] Z. Song and A. Dogandžić, "A max-product EM algorithm for reconstructing Markov-tree sparse signals from compressive samples," *IEEE Transactions on Signal Processing*, vol. 61, no. 23, pp. 5917–5931, 2013.
- [4] Y. Ueng, K. Liao, H. Chou, and C. Yang, "A high-throughput trellis-based layered decoding architecture for non-binary LDPC codes using max-log-QSPA," *IEEE Transactions on Signal Processing*, vol. 61, no. 11, pp. 2940–2951, 2013.
- [5] B. Mor, S. Garhwal, and A. Kumar, "A systematic review of hidden Markov models and their applications," *Archives of Computational Methods in Engineering*, 2020.
- [6] B. H. Juang and L. R. Rabiner, "Hidden Markov models for speech recognition," *Technometrics*, vol. 33, no. 3, pp. 251–272, 1991.
- [7] A. A. Salah, M. Bicego, L. Akarun, E. Grosso, and M. Tistarelli, "Hidden Markov model-based face recognition using selective attention," in *Human Vision and Electronic Imaging XII*, vol. 6492, International Society for Optics and Photonics. SPIE, 2007, pp. 404–412.
- [8] A. Krogh, B. Larsson, G. Von Heijne, and E. L. Sonnhammer, "Predicting transmembrane protein topology with a hidden Markov model: application to complete genomes," *Journal of molecular biology*, vol. 305, no. 3, pp. 567–580, 2001.
- [9] L. Pan, M. W. Marcellin, W. E. Ryan, and B. Vasic, "Viterbi detection for compressively sampled FHSS-GFSK signals," *IEEE Transactions on Signal Processing*, vol. 63, no. 22, pp. 5965–5975, 2015.
- [10] Y. Yang, S. Chen, M. A. Maddah-Ali, P. Grover, S. Kar, and J. Kovačević, "Fast temporal path localization on graphs via multiscale Viterbi decoding," *IEEE Transactions on Signal Processing*, vol. 66, no. 21, pp. 5588–5603, 2018.
- [11] T. Long, L. Zheng, X. Chen, Y. Li, and T. Zeng, "Improved probabilistic multi-hypothesis tracker for multiple target tracking with switching attribute states," *IEEE Transactions on Signal Processing*, vol. 59, no. 12, pp. 5721–5733, 2011.
- [12] P. Di Viesti, G. M. Vitetta, and E. Sirignano, "Double Bayesian smoothing as message passing," *IEEE Transactions on Signal Processing*, vol. 67, no. 21, pp. 5495–5510, 2019.
- [13] A. Viterbi, "Error bounds for convolutional codes and an asymptotically optimum decoding algorithm," *IEEE transactions on Information Theory*, vol. 13, no. 2, pp. 260–269, 1967.
- [14] Y. Lifshits, S. Mozes, O. Weimann, and M. Ziv-Ukelson, "Speeding up HMM decoding and training by exploiting sequence repetitions," *Algorithmica*, vol. 54, no. 3, pp. 379–399, 2009.
- [15] A. Sand, C. N. Pedersen, T. Mailund, and A. T. Brask, "HMMlib: A C++ library for general hidden Markov models exploiting modern CPUs," in *2010 Ninth International Workshop on Parallel and Distributed Methods in Verification, and Second International Workshop on High Performance Computational Systems Biology*. IEEE, 2010, pp. 126–134.
- [16] J. Nielsen and A. Sand, "Algorithms for a parallel implementation of hidden Markov models with a small state space," in *2011 IEEE International Symposium on Parallel and Distributed Processing Workshops and Phd Forum*. IEEE, 2011, pp. 452–459.

- [17] S. Chatterjee and S. Russell, "A temporally abstracted Viterbi algorithm," in *Proceedings of the Twenty-Seventh Conference on Uncertainty in Artificial Intelligence*, 2011, p. 96–104.
- [18] Zhihui Du, Zhaoming Yin, and D. A. Bader, "A tile-based parallel Viterbi algorithm for biological sequence alignment on GPU with CUDA," in *2010 IEEE International Symposium on Parallel Distributed Processing, Workshops and Phd Forum (IPDPSW)*, 2010, pp. 1–8.
- [19] S. Maleki, M. Musuvathi, and T. Mytkowicz, "Parallelizing dynamic programming through rank convergence," *ACM SIGPLAN Notices*, vol. 49, no. 8, pp. 219–232, 2014.
- [20] J. D. Owens, M. Houston, D. Luebke, S. Green, J. E. Stone, and J. C. Phillips, "GPU computing," *Proceedings of the IEEE*, vol. 96, no. 5, pp. 879–899, 2008.
- [21] H. Esmailzadeh, A. Sampson, L. Ceze, and D. Burger, "Neural acceleration for general-purpose approximate programs," in *2012 45th Annual IEEE/ACM International Symposium on Microarchitecture*, 2012, pp. 449–460.
- [22] N. P. Jouppi, C. Young, N. Patil, D. Patterson, G. Agrawal, R. Bajwa, S. Bates, S. Bhatia, N. Boden, A. Borchers *et al.*, "In-datacenter performance analysis of a tensor processing unit," in *Proceedings of the 44th Annual International Symposium on Computer Architecture*, 2017, pp. 1–12.
- [23] D. Luebke, "CUDA: Scalable parallel programming for high-performance scientific computing," in *2008 5th IEEE International Symposium on Biomedical Imaging: From Nano to Macro*, 2008, pp. 836–838.
- [24] G. E. Blelloch, "Scans as primitive parallel operations," *IEEE Transactions on Computers*, vol. 38, no. 11, pp. 1526–1538, 1989.
- [25] —, "Prefix sums and their applications," School of Computer Science, Carnegie Mellon University, Tech. Rep. CMU-CS-90-190, 1990.
- [26] J. Li, S. Chen, and Y. Li, "The fast evaluation of hidden Markov models on GPU," in *2009 IEEE International Conference on Intelligent Computing and Intelligent Systems*, vol. 4. IEEE, 2009, pp. 426–430.
- [27] C. Liu, "cuHMM: a CUDA implementation of hidden Markov model training and classification," Johns Hopkins University, Tech. Rep., 2009.
- [28] D. Zhang, R. Zhao, L. Han, T. Wang, and J. Qu, "An implementation of Viterbi algorithm on GPU," in *2009 First International Conference on Information Science and Engineering*. IEEE, 2009, pp. 121–124.
- [29] S. Hymel, "Massively parallel hidden Markov models for wireless applications," Ph.D. dissertation, Virginia Tech, 2011.
- [30] S. Särkkä and Á. F. García-Fernández, "Temporal parallelization of Bayesian smoothers," *IEEE Transactions on Automatic Control*, vol. 66, no. 1, pp. 299–306, 2021.
- [31] F. Yaghoobi, A. Corenflos, S. Hassan, and S. Särkkä, "Parallel iterated extended and sigma-point Kalman smoothers," in *To appear in Proceedings of IEEE International Conference on Acoustics, Speech and Signal Processing (ICASSP)*, 2021.
- [32] S. Särkkä, *Bayesian Filtering and Smoothing*. Cambridge University Press, 2013.
- [33] D. Koller and N. Friedman, *Probabilistic Graphical Models: Principles and Techniques*. MIT Press, 2009.
- [34] S. Rangan, A. K. Fletcher, V. K. Goyal, E. Byrne, and P. Schniter, "Hybrid approximate message passing," *IEEE Transactions on Signal Processing*, vol. 65, no. 17, pp. 4577–4592, 2017.
- [35] Y. Weiss, "Correctness of local probability propagation in graphical models with loops," *Neural computation*, vol. 12, no. 1, pp. 1–41, 2000.
- [36] L. Rabiner and B. Juang, "An introduction to hidden Markov models," *IEEE ASSP magazine*, vol. 3, no. 1, pp. 4–16, 1986.
- [37] J. Pearl, *Probabilistic reasoning in intelligent systems: networks of plausible inference*. Morgan Kaufmann, 1988.
- [38] G. Shafer and P. Shenoy, "Probability propagation," *Annals of Mathematics and Artificial Intelligence*, vol. 2, p. 327–351, 1990.
- [39] C. M. Bishop, *Pattern Recognition and Machine Learning*. Springer, 2006.
- [40] R. G. Cowell, P. Dawid, S. L. Lauritzen, and D. J. Spiegelhalter, *Probabilistic networks and expert systems: Exact computational methods for Bayesian networks*. Springer, 2006.
- [41] B. J. Frey, J. F. Brendan, and B. J. Frey, *Graphical models for machine learning and digital communication*. MIT press, 1998.
- [42] R. Larson and J. Peschon, "A dynamic programming approach to trajectory estimation," *IEEE Transactions on Automatic Control*, vol. 11, no. 3, pp. 537–540, July 1966.
- [43] L. E. Baum, T. Petrie, G. Soules, and N. Weiss, "A maximization technique occurring in the statistical analysis of probabilistic functions of Markov chains," *The annals of mathematical statistics*, vol. 41, no. 1, pp. 164–171, 1970.
- [44] A. P. Dempster, N. M. Laird, and D. B. Rubin, "Maximum likelihood from incomplete data via the EM algorithm," *Journal of the Royal Statistical Society: Series B (Methodological)*, vol. 39, no. 1, pp. 1–22, 1977.
- [45] M. Abadi *et al.*, "TensorFlow: Large-scale machine learning on heterogeneous systems," 2015, software available from tensorflow.org. [Online]. Available: <https://www.tensorflow.org/>